Sidelobe Levels, Aperture Efficiency and Sensitivity Comparisons of Axisymmetric and Asymmetric Antennas

S. Srikanth
National Radio Astronomy Observatory

June 27, 1989

I. Introduction

The baseline instrument as suggested in the formal proposal to the NSF for the new Green Bank telescope is an axisymmetric cassegrain antenna. At the Green Bank workshop in December 1988 [1], among the desired characteristics laid out for the new antenna, the requirement for improving the far sidelobe response and reducing reflections within the antenna was discussed extensively. This has led to the decision to continue study of an unblocked asymmetric antenna. Lately, F. J. Lockman [2] has dealt with the consequences of aperture blockage on astronomical observations in detail. This memorandum presents quantitative results for comparison based on a numerical study of the two designs.

II. Features of the Comparison

Listed below are the features of the softwares used and assumptions made in the comparison:

1) The study is based on a cassegrain system, paraboloid main reflector and hyperboloid subreflector.

2) The analyses were done using a Reflector Antenna Code [3], [4], and a Spherical Wave Expansion/Physical Optics Scattering Program (SW/PO) [5], provided by JPL. The subreflector far-field pattern is calculated using the SW/PO program, where the incident field pattern of the feed is represented by spherical wave expansion. In [5] Ludwig has shown that using the above method, the computed and measured patterns from a hyperboloid subreflector were in good agreement down to -35 dB and even through the first sidelobe. For the configurations to be presented next, the main reflector is in the near field of the subreflector at the analysis frequencies. Using the subreflector far-field pattern as input into the SW/PO program, the near-field pattern at a distance equal to the primary focal length is calculated. This is used as the incident pattern on the main reflector in the Reflector Antenna Code to calculate the secondary field pattern of the cassegrain antenna. In the Reflector Antenna Code, the secondary field accounts for the reflected field, the diffracted field from the edge of the main reflector, the scattered field from the subreflector support structure and the blocked field due to the subreflector. The scattered field from the support struts is the plane wave scattered field, while the

spherical wave scattered field is not included. Also, the subreflector edge diffraction is not accounted for.

3) The configurations for the two antennas are shown in Figures 1 and 2. For the axisymmetric antenna, a primary focal length to diameter ratio (f/D) of 0.40 has been used. The main and subreflector diameters are 100 meters and 7 meters, respectively. This axisymmetric antenna is compared with asymmetric antennas of projected aperture diameters of 100 meters and 90 meters. For the asymmetric antenna, a f/D of 0.615, about where the beam efficiency is at its peak value [6], is used. This value is also close to the optimum for mechanical reasons [7]. The subreflector diameters are 7.6 and 6.97 meters for the 100 and 90 meter asymmetric antennas, respectively.

4) For the axisymmetric antenna, the tripod focal support structure proposed by L. King has been used. The cross-section of each pod is a trapezoidal box-type structure 35" x 19" x 146". This structure has about 2.5% blockage and 0.77 Hz natural frequency. In case of the asymmetric antenna, the support tower for the subreflector is not included in the analysis, as dimensions for the tower were not available.

5) For the asymmetric antenna, a dual offset configuration (Figure 2(b) in [8]) has been used. The tilt angles of the feed with respect to the hyperboloid axis and of the hyperboloid axis with respect to the paraboloid axis have been chosen for a rotationally symmetric aperture distribution as in [9].

6) The comparisons are done at frequencies of 1.4 GHz and 4.8 GHz. Reducing the stray radiation entering through the sidelobes in HI observations of the 21 cms line is one of the prime motivations for the asymmetric configuration. Hence, the frequency of 1.4 GHz at which the 7-meter subreflector is about 33 wavelengths in diameter. Above 4.8 GHz, the size of the main reflector becomes enormous in wavelengths. The array dimensions could not be increased any further in the Reflector Antenna Code without computer overflow and, hence, set the upper frequency limit at 4.8 GHz.

7) The half angle from the secondary focus to the subreflector edge for both axisymmetric and asymmetric antennas is 7.14°, where the feed pattern is -13.5 dB down. The subreflector pattern has a taper of -15.8 dB at 1.4 GHz and -16.8 dB at 4.8 GHz at the edge of the main reflector for the axisymmetric antenna. While, for the asymmetric antenna, the edge tapers at the two frequencies are given in Table 1. The edges referred to are in the plane of the paper (symmetric plane of the antenna) in Figure 2.

TABLE 1. Subreflector Pattern Taper at the Edge of the Main Reflector

Frequency (GHz)	100-Meter Asymmetric Top Edge (dB)	100-Meter Asymmetric Bottom Edge (dB)	90-Meter Asymmetric Top Edge (dB)	90-Meter Asymmetric Bottom Edge (dB)
1.4	-16.6	-19.4	-14.7	-19.0
4.8	-16.9	-19.9	-16.6	-19.7

III. Copolar Sidelobe Response

The far-field patterns of the axisymmetric antenna at 1.4 GHz are given in Figure 3. In Figure 3(a) strut scattered field and effect of blockage by the subreflector are not present. Figures 3(b), 3(c) and 3(d) show the field patterns with aperture blockage in a strut plane, and planes 15° and 30° from the strut plane, respectively. Figure 4 gives similar patterns at 4.8 GHz. The aperture blockage reduces the gain by 0.2 dB at both frequencies and raises the sidelobe envelope on the average by 22 dB at 1.4 GHz and 30 dB at 4.8 GHz in the strut plane and 18 and 14 dB at 1.4 and 4.8 GHz, respectively, in the 30° plane. The sidelobe specification curve of 32 dBi - (25 dBi) log(θ) (1° $\leq \theta \leq$ 48°) and -10 dBi ($\theta >$ 48°), where θ is the angle in degrees from the main beam direction, recommended by CCIR is depicted in broken lines for comparison. At 4.8 GHz the sidelobes in the 30° plane (θ = 10 to 100°) lie between 12 and 27 dB below the CCIR curve, while in the strut plane the sidelobes are barely below the curve up to θ = 40° and even exceed the curve at certain azimuth angles. At 1.4 GHz the sidelobe peaks have moved closer to the CCIR curve in the 15° and 30° planes, while in the strut plane remains at the same level as at 4.8 GHz. The isolated peaks seen in the 15° and 30° planes near about θ = 70° at both frequencies are due to the overlapping of the scattering cones from adjacent struts. The cross-section of the tripod was increased by 4", and its effect was an increase in the level of the sidelobe peaks by about 5 dB in azimuth angles up to 10°. The discontinuity seen in the above patterns at θ = 100° is due to the absence of second-order diffraction terms in the Reflector Antenna Code.

In the following section, it is shown that the sensitivity of a 90-meter asymmetric antenna is nearly equal to that of the 100-meter axisymmetric antenna. Hence, only the 90-meter asymmetric antenna patterns are included in this memo. The sidelobe levels with respect to isotropic of the 100-meter and 90-meter asymmetric antennas are about the same. However, the gain of the 100-meter antenna is about 0.8 dB greater than the 90-meter antenna.

Figure 5 gives the far-field patterns for the asymmetric 90-meter antenna in its asymmetric plane and 30°, 45° and 80° from this plane at 1.4 GHz. Figure 6 shows patterns at 4.8 GHz. The sidelobe peaks are about 27 dB below the CCIR curve in all the planes at 1.4 GHz and between 30 and 35 dB below at 4.8 GHz. Comparing this with the axisymmetric antenna, the sidelobe envelope of the asymmetric antenna is about 30 dB below that of the axisymmetric antenna in the strut plane and about 20 dB lower in other planes. However, in this comparison, it is to be noted that spherical wave scattered field by the struts in the axisymmetric antenna have not been included. L. King's proposed struts are designed to keep the spherical blockage to a minimum and may be comparable to the bent struts [10], [11]. It is hard to predict how much the near sidelobes would increase if spherical wave scattering is included. Again, if Lee would increase the cross-section of the pod box, for reasons of increasing the natural frequency, the sidelobe levels for the axisymmetric antenna would further move up closer to the CCIR curve. Regarding the asymmetric antenna, the tower supporting the subreflector, which is outside the projected aperture, if included, may increase the sidelobe level by about 5 dB. For the asymmetric antenna, the patterns in its symmetric plane could not be computed for reasons of memory overflow in the Convex. The sidelobe levels in the symmetric plane are expected to be the same as in the other planes shown in Figures 5 and 6, except the backlobes at azimuth angles between 100° and 150° are predicted to be about 35 dB below isotropic at 1.4 GHz and 45 dB at 4.8 GHz.

IV. Cross-Polar Sidelobes

The sidelobe patterns are not shown in the memo. However, for the axisymmetric antenna, the sidelobes in the strut planes exceed the CCIR curve at several azimuth angles in the range of $\theta = 30°$ to $100°$ at 4.8 GHz. At 1.4 GHz, there are only two peaks exceeding the reference curve. For the 90-meter asymmetric antenna, there is only one sidelobe at approximately $\theta = 90°$ which exceeds the CCIR curve in the plane 80° from the asymmetric plane of the antenna. As one moves towards the asymmetric plane, this sidelobe moves further out from the main beam direction. This is independent of frequency. The rest of the sidelobe envelope is at least 30 dB below the CCIR curve.

V. Aperture Efficiency and Sensitivity

An attempt has been made to compute the gain and sensitivity of either type of antenna in this memo. The gain of an aperture antenna is given by

$$G = \frac{4\pi\ A\ \eta_a}{\lambda^2}$$

a dimensionless quantity, where A is the physical aperture, η_a is the aperture efficiency, and λ is the wavelength. The sensitivity is given by G/T, where T is the total system temperature given by

$$T = T_{rx} + T_{sky} + T_{ant} \ .$$

For estimating the system temperature, the receiver temperature is taken at 7° K and 10° K at 1.4 GHz and 4.8 GHz, respectively [12]. For T_{sky}, a value of 6° K is used. T_{ant} is comprised of scattered and spillover temperatures. The scattered temperature for a quadrupod in a cassegrain antenna is expected to be around 3° K at zenith and 5.5° K at 30° elevation [13]. Spillover, which would be nearly equal for the axisymmetric and asymmetric antennas, is fixed at 3° K at 1.4 GHz and 2° K at 4.8 GHz, as in the VLBA project book.

The aperture efficiency, which is a measure of how efficiently the physical area of the antenna is used, is a product of a number of efficiencies and given as

$$\eta_a = \eta_{ill} \cdot \eta_{bl} \cdot \eta_{sp} \cdot \eta_{surf} \cdot \eta_{misc} \ .$$

Table 2 gives the various efficiencies at both frequencies. The illumination efficiency η_{ill} and blockage efficiency η_{bl} are computed from the gain outputs of the Reflector Antenna Code. The spillovers past the subreflector and the main reflector have been computed from the Physical Optics program and denoted as η_{sps} and η_{spm}, respectively. The efficiency loss due to phase errors in the aperture field caused by random surface errors is accounted for by the factor η_{surf}. For calculating this factor, rms surface deviations of 0.25 mm for the main reflector with active surface control and 0.15 mm for the subreflector have been used. The factor η_{misc}, which accounts for losses due to reflections in the antenna, resistive losses, etc. is about 0.95 for the axisymmetric antenna. For the asymmetric case, since reflections are negligible (about 30 dB less than the axisymmetric antenna), η_{misc} is taken to be 0.955. The aperture efficiency, gain, system temperature and G/T are tabulated in Table 2 for the 100-meter axisymmetric antenna, and the 100-meter and 90-meter asymmetric antennas. It is seen from the last column that the sensitivity of a 90-meter asymmetric antenna is nearly equal to the 100-meter axisymmetric antenna.

VI. Summary

The 90-meter asymmetric antenna is expected to have the same sensitivity as that of a 100-meter axisymmetric antenna. R. Norrod in [12] has also arrived at the same conclusion. The cost of building either one appears to be almost equal. Hence, for the same cost and sensitivity, the asymmetric antenna would give us 20 to 30 dB lower sidelobe response. Further, an asymmetric antenna built in the radio quiet zone at Green Bank will be a state-of-the-art, unique instrument. Further analyses accounting for spherical wave scattering for the axisymmetric antenna and including the effects of the cantilever tower for the asymmetric antenna need to be done. We could have the computations done with more advanced software, if available, either at JPL or at Ohio State University for getting more confidence in the numbers calculated in this memo.

<u>References</u>:

[1] "Proceedings of a Green Bank Workshop," NRAO, December 2-3, 1988.

[2] F. J. Lockman, "On Aperture Blockage and its Consequences for Astronomical Observations," NRAO NLSRT Memo No. 60, May 1989.

[3] R. C. Rudduck and Y. C. Chang, "Numerical Electromagnetic Code - Reflector Antenna Code, NEC-REF (Version 2) Part I: User's Manual," The Ohio State University Electro-Science Laboratory, Dec. 1982.

[4] Y. C. Chang and R. C. Rudduck, "Numerical Electromagnetic Code - Reflector Antenna Code, NEC-REF (Version 2) Part II: Code Manual," The Ohio State University Electro-Science Laboratory, Dec. 1982.

[5] A. Ludwig, "Calculation of Scattered Patterns from Asymmetrical Reflectors," Technical Report 32-1430, Jet Propulsion Laboratory, Pasadena, CA, Feb. 15, 1970.

[6] S. Srikanth, "Numerical Analysis of Offset Reflector Antennas," NRAO Technical Study Group Report #10, Jan. 5, 1989.

[7] A. R. Thompson, "Possible Feasible Approaches to the Design of a Large Offset Feed Radio Telescope," NRAO NLSRT Memo No. 43, Dec. 1988.

[8] A. W. Rudge and N. A. Adatia, "Offset-Parabolic-Reflector Antennas: A Review," <u>Proc. of the IEEE</u>, vol. 66, no. 12, pp. 1592-1618, 1978.

[9] C. J. Sletten, <u>Reflector and Lens Antennas, Analysis and Design Using Personal Computers</u>, Artech House, 1988.

[10] G. Schindler, "Reduction of Sidelobe Level by Improved Strut Design for Low F/D Cassegrain Antennas," <u>Electronic Letters</u>, vol. 21, no. 5, pp. 203-204, Feb. 28, 1985.

[11] H. Thielen, V. Hombach, and G. Schindler, "Reflector Antennas with Bent Struts," <u>IEEE/AP-S Int. Symp. Digest</u>, pp. 173-176, June 1985.

[12] R. Norrod, "Comparisons of Symmetric and Asymmetric Antennas," NRAO NLSRT Memo No. 54, May 1989.

[13] T. Verruttipong, V. Galindo-Israel and W. A. Imbriale, "Low-Loss Offset Feeds for Electrically-Large, Symmetric, Dual-Reflector Antennas," <u>IEEE Transaction on A&P</u>, vol. AP-35, no. 7, pp. 745-755, July 1987.

TABLE 2. Aperture Efficiency and G/T Comparison of Axisymmetric and Asymmetric Antennas

Antenna	Freq. (GHz)	η_{ill}	η_{bl}	η_{sps}	η_{spm}	η_{misc}	η_{surf}	η_a	G (dB)	T (°K) At Elevation		G/T (dB) At Elevation	
										90°	30°	90°	30°
Axisym. 100-m	1.4	0.7570	0.9572	0.9614	0.9914	0.95	0.9997	0.6559	61.6172	19	21.5	48.8296	48.2928
	4.8	0.7541	0.9572	0.9636	0.9950	0.95	0.9965	0.6552	72.2791	21	23.5	59.0570	58.5685
Asymm. 100-m	1.4	0.7331	1	0.9617	0.9926	0.955	0.9997	0.6681	61.6973	16	16	49.6561	49.6561
	4.8	0.7302	1	0.9636	0.9955	0.955	0.9965	0.6666	72.3540	18	18	59.8013	59.8013
Asymm. 90-m	1.4	0.7339	1	0.9618	0.9927	0.955	0.9997	0.6690	60.7878	16	16	48.7466	48.7466
	4.8	0.7311	1	0.9634	0.9955	0.955	0.9965	0.6673	71.4433	18	18	58.8906	58.8906

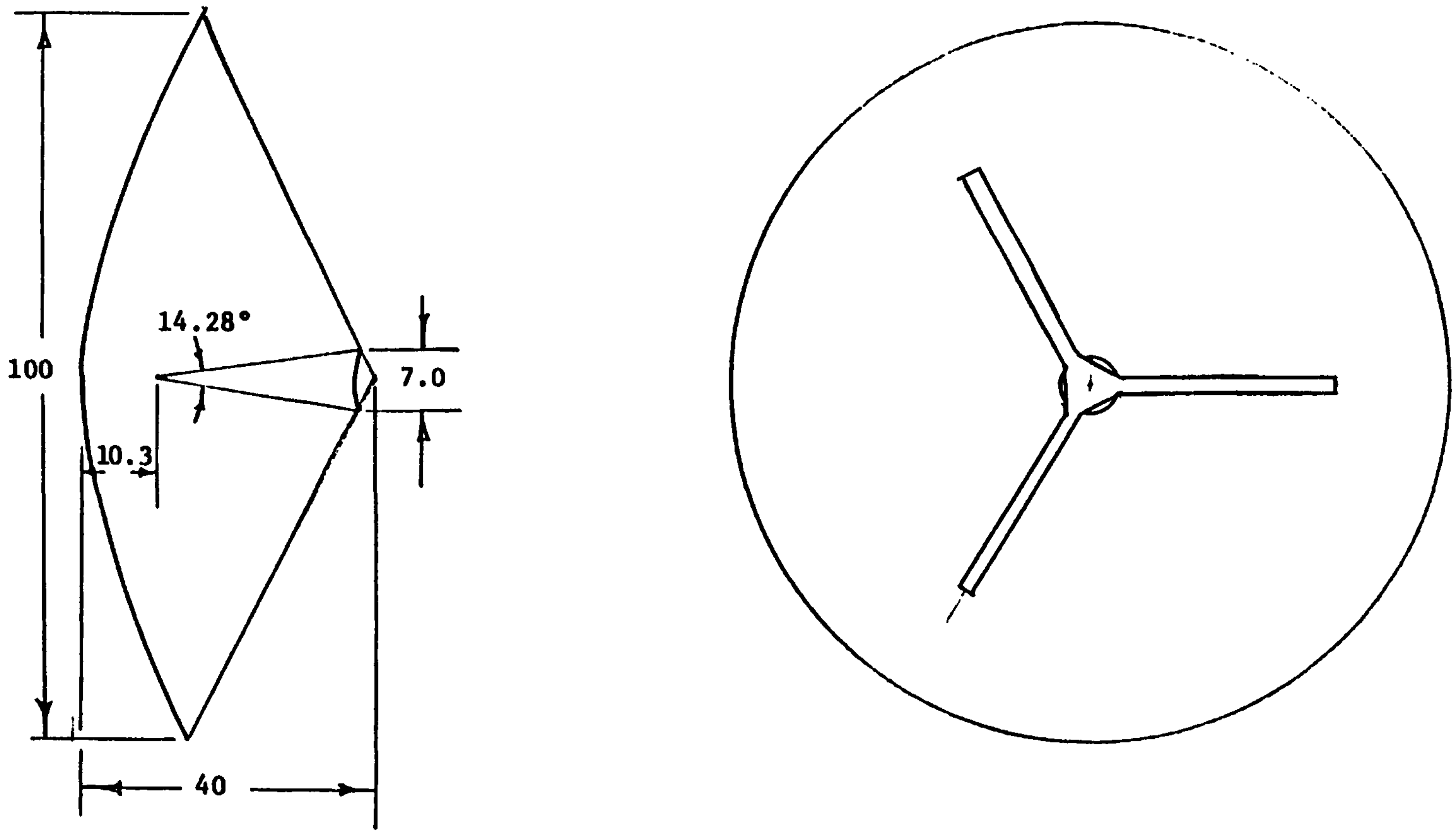

All dimensions in meters except as noted.

Fig. 1. 100-meter axisymmetric antenna.

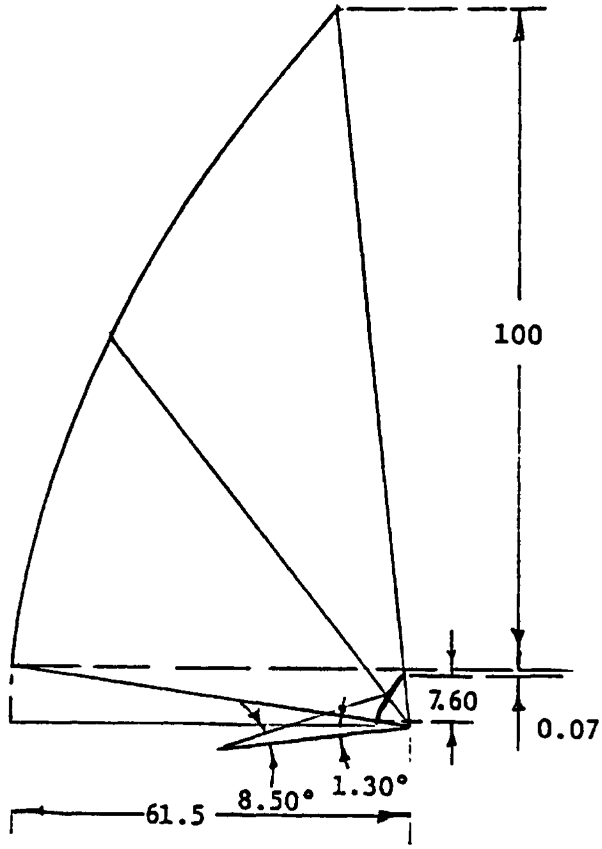

Fig. 2(a). 100-meter asymmetric antenna.

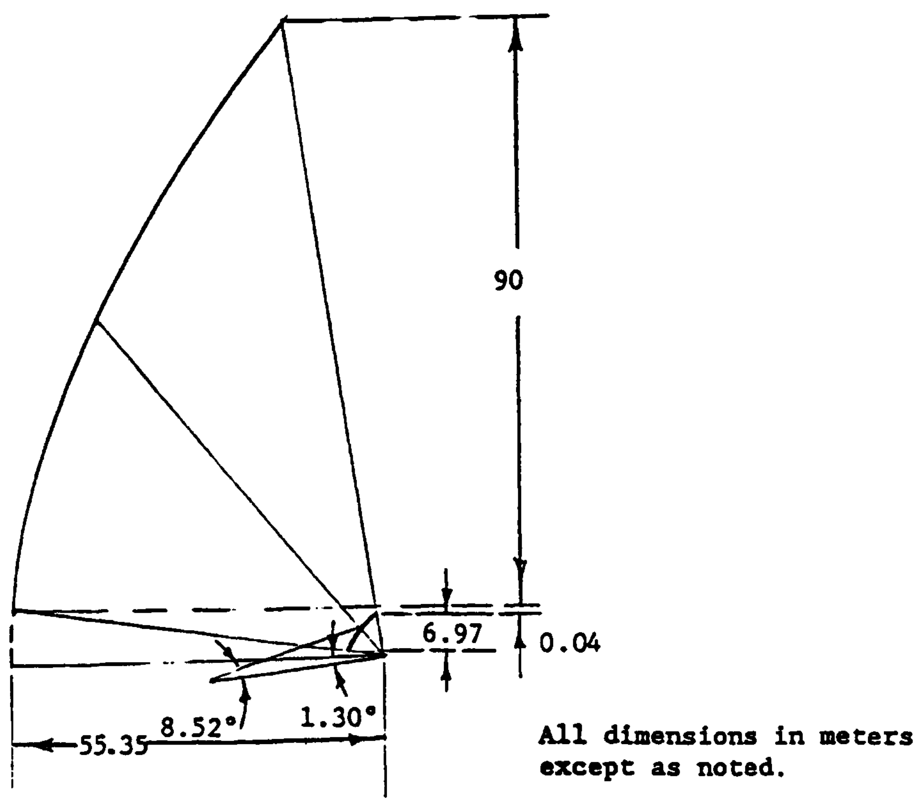

Fig. 2(b). 90-meter asymmetric antenna.

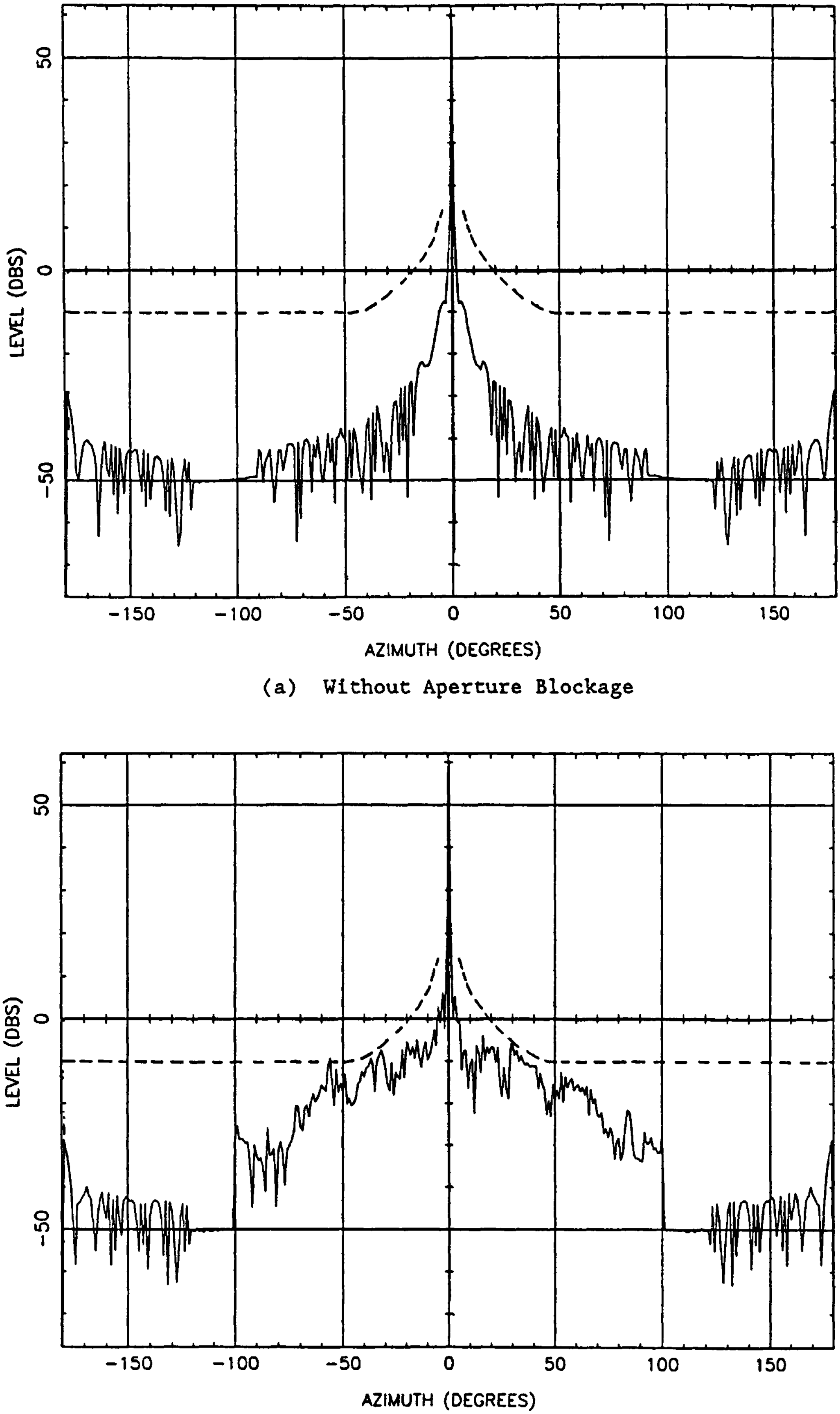

(a) Without Aperture Blockage

(b) With Blockage - Strut (0°) Plane

Fig. 3. Pattern of 100-meter axisymmetric antenna at 1.4 GHz.

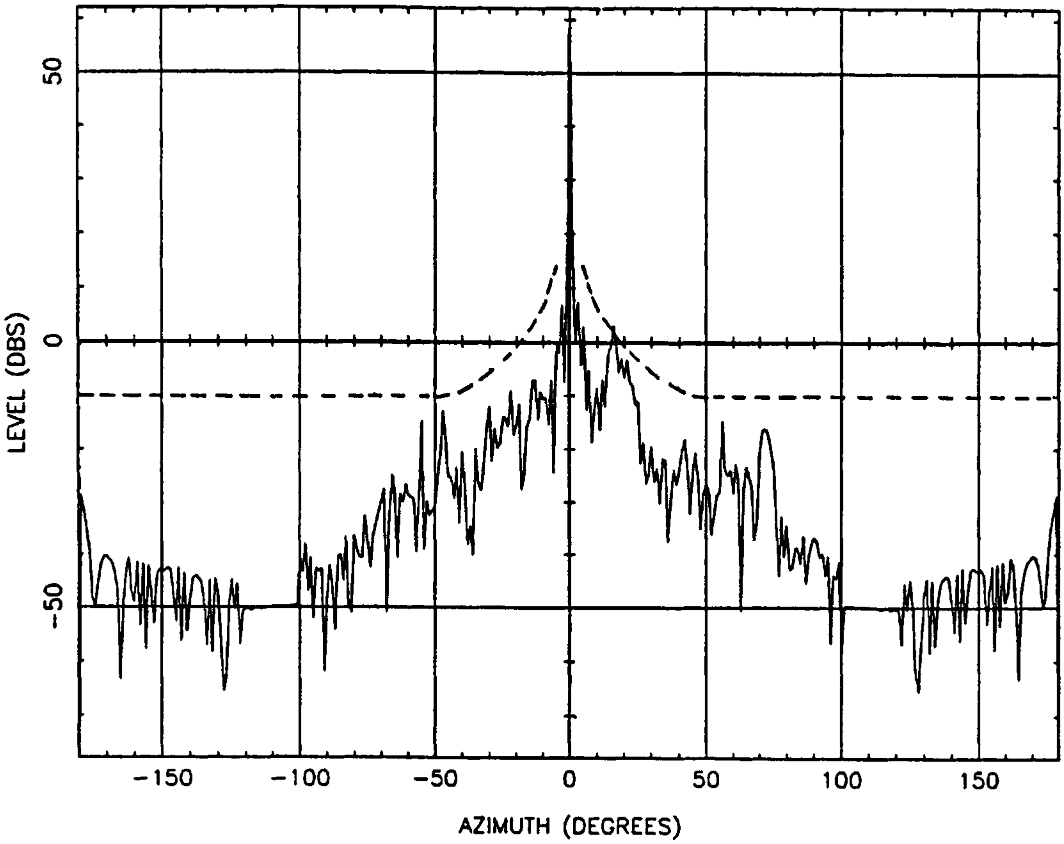

(c) With Blockage - 15° Plane

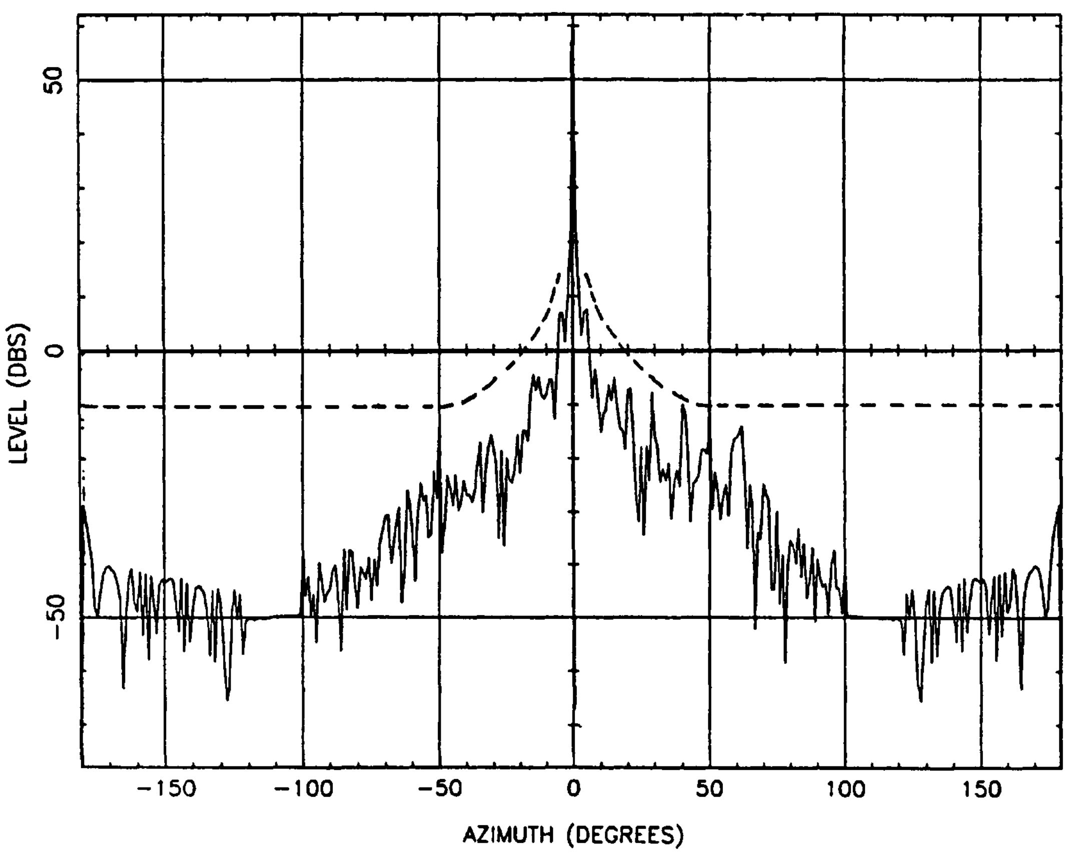

(d) With Blockage - 30° Plane

Fig. 3. Pattern of 100-meter axisymmetric antenna at 1.4 GHz.

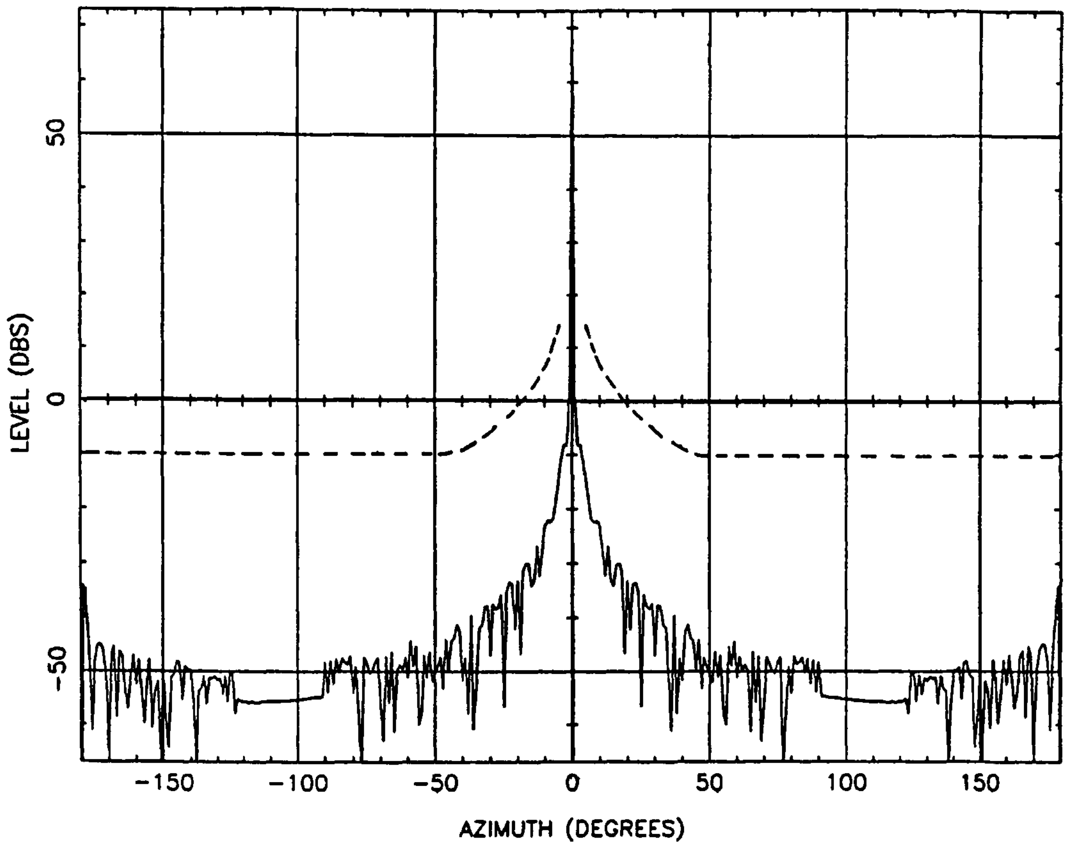

(a) Without Aperture Blockage

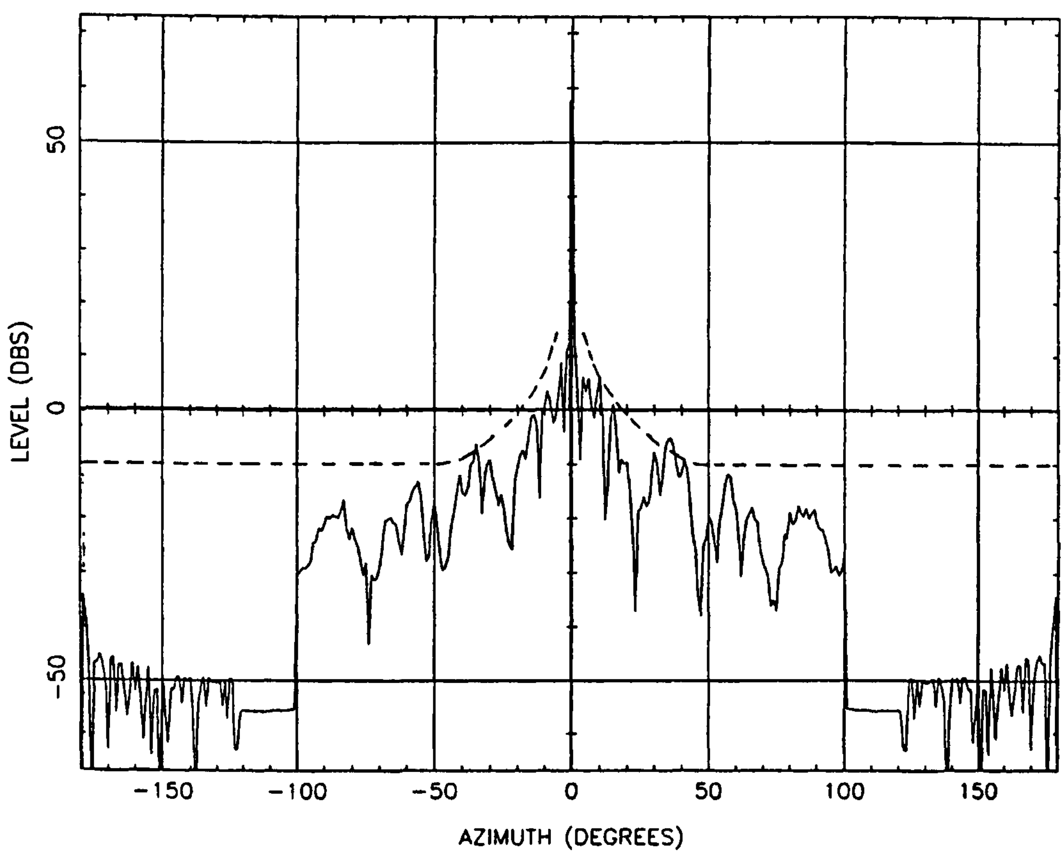

(b) With Blockage - Strut (0°) Plane

Fig. 4. Pattern of 100-meter axisymmetric antenna at 4.8 GHz.

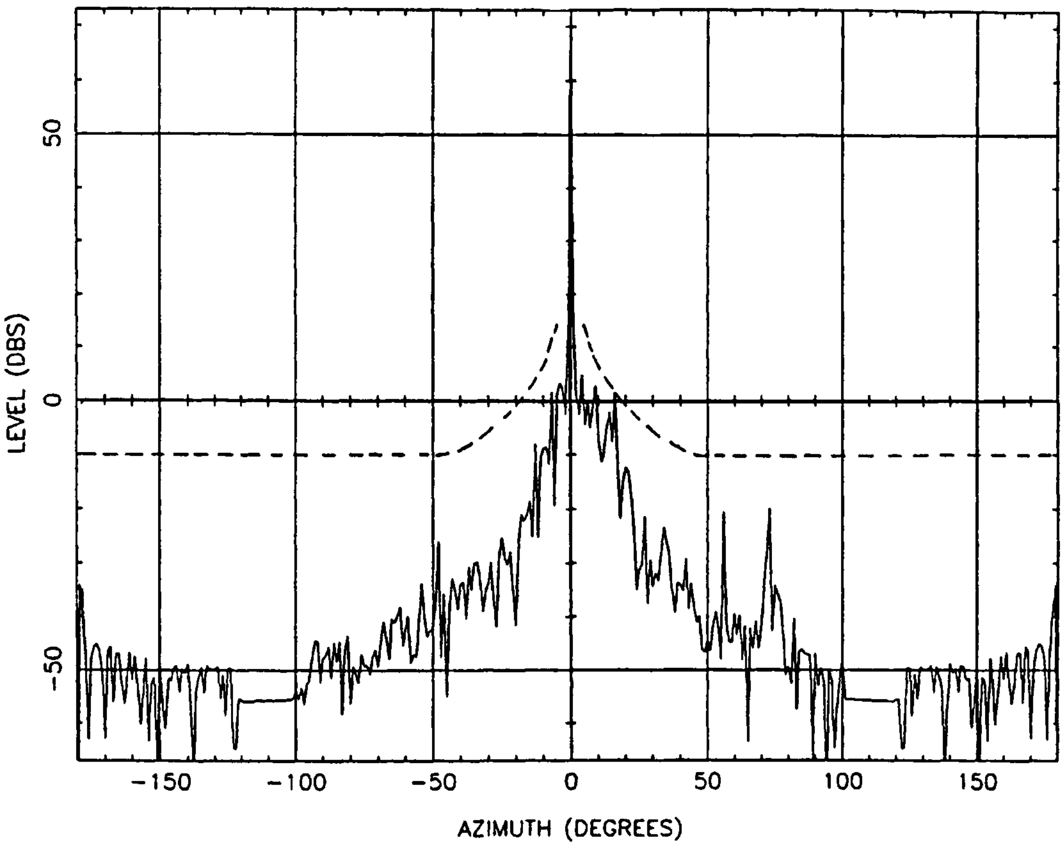

(c) With Blockage - 15° Plane

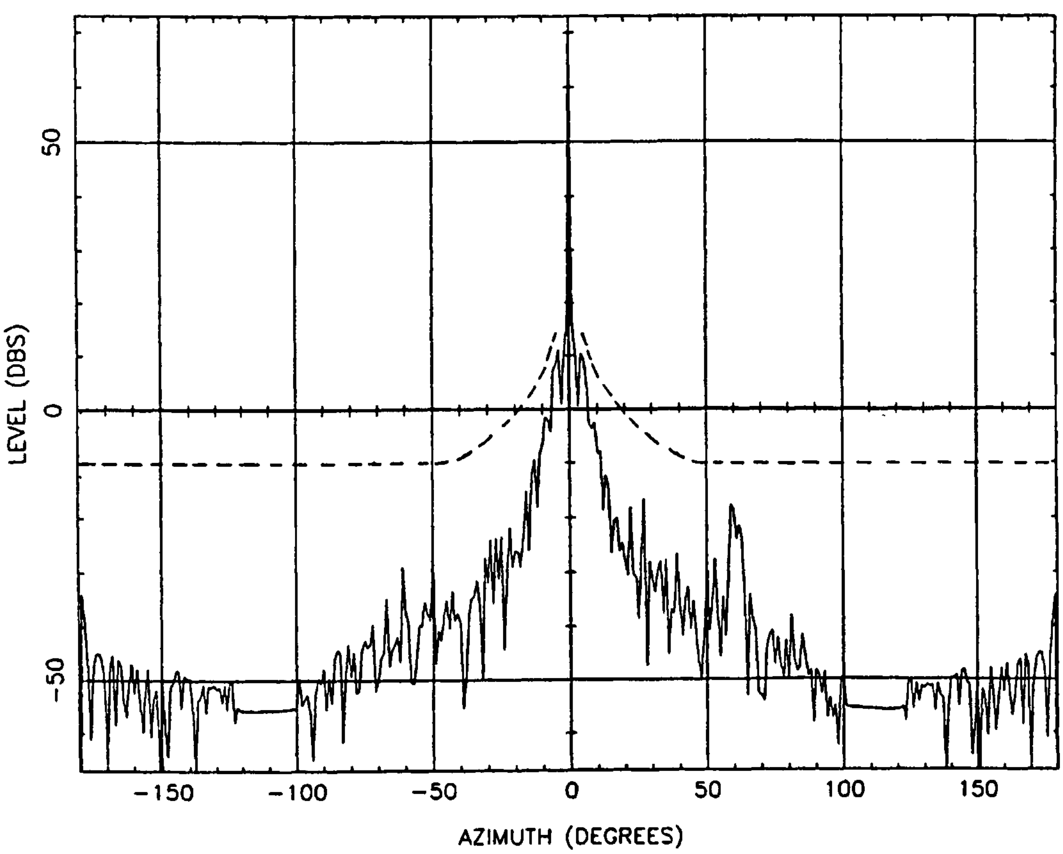

(d) With Blockage - 30° Plane

Fig. 4. Pattern of 100-meter axisymmetric antenna at 4.8 GHz.

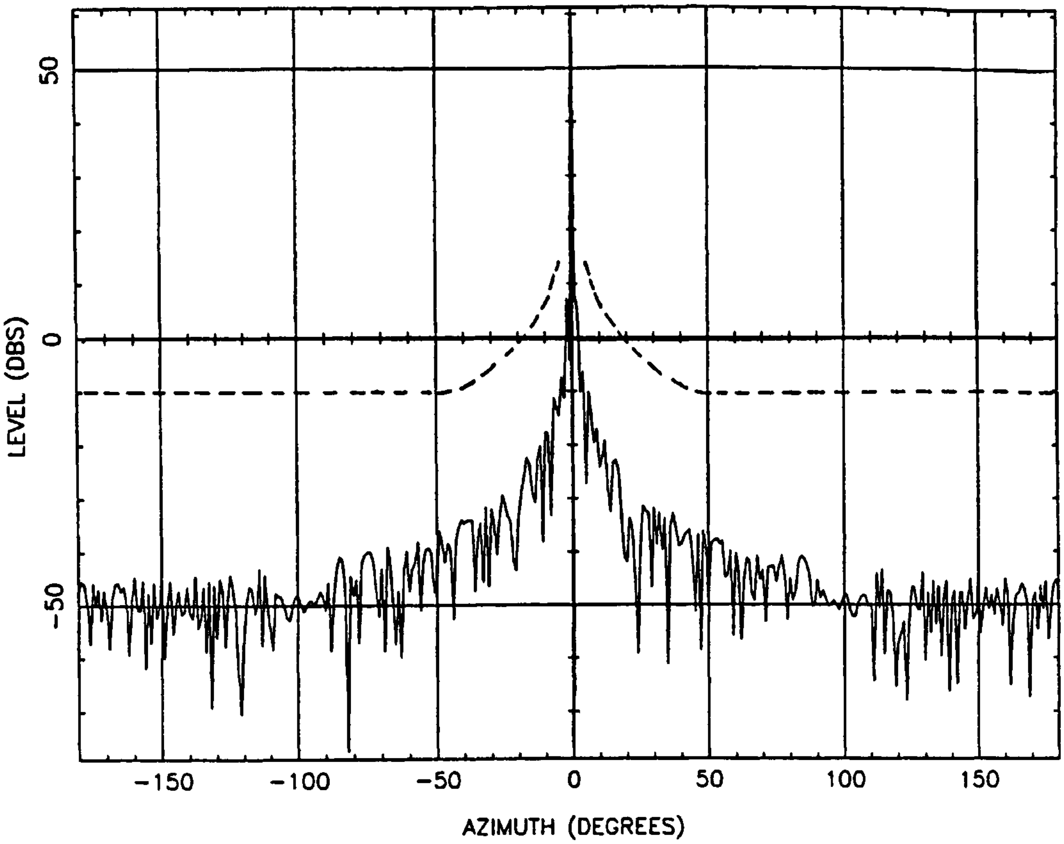

(a) Asymmetric (0°) Plane

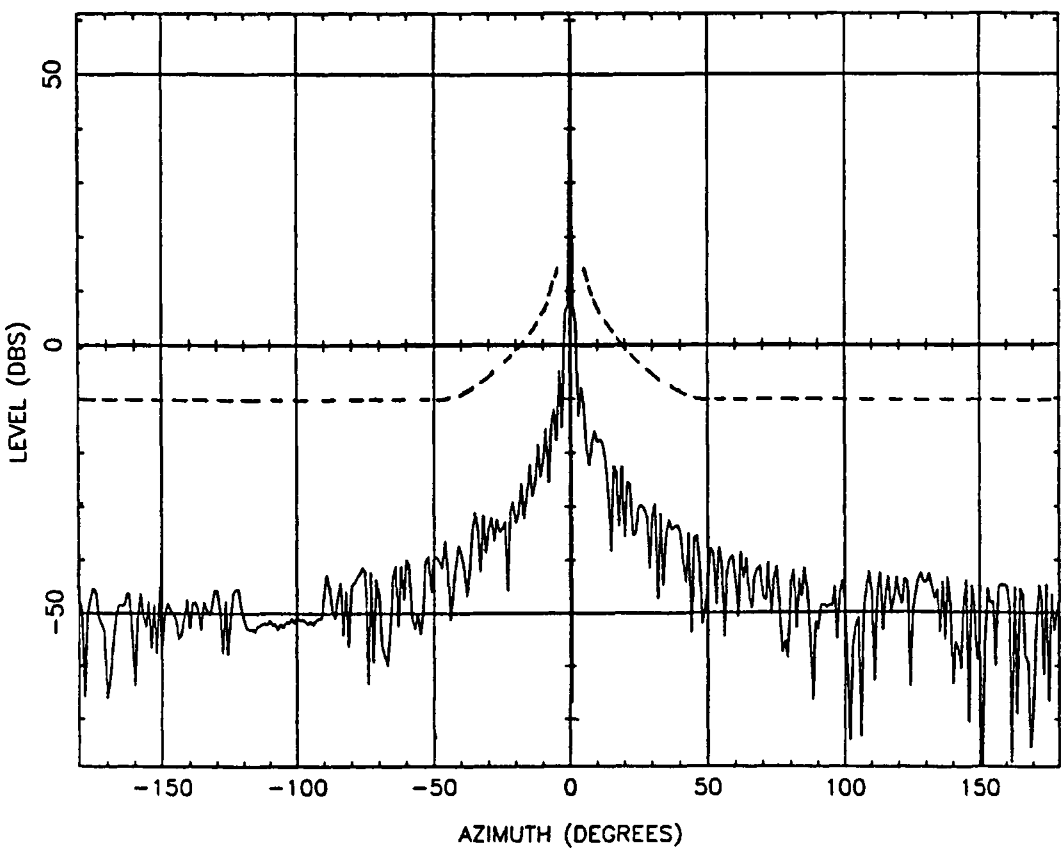

(b) 30° Plane

Fig. 5. Pattern of 90-meter asymmetric antenna at 1.4 GHz.

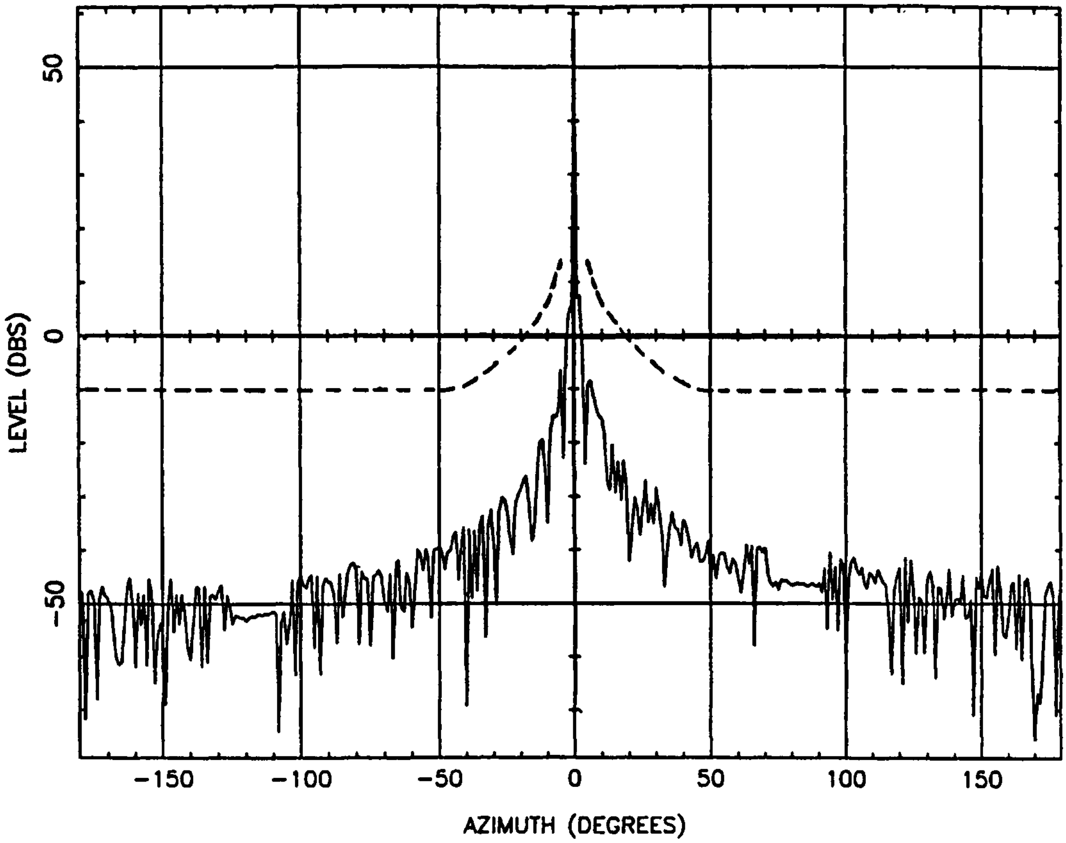

(c) 45° Plane

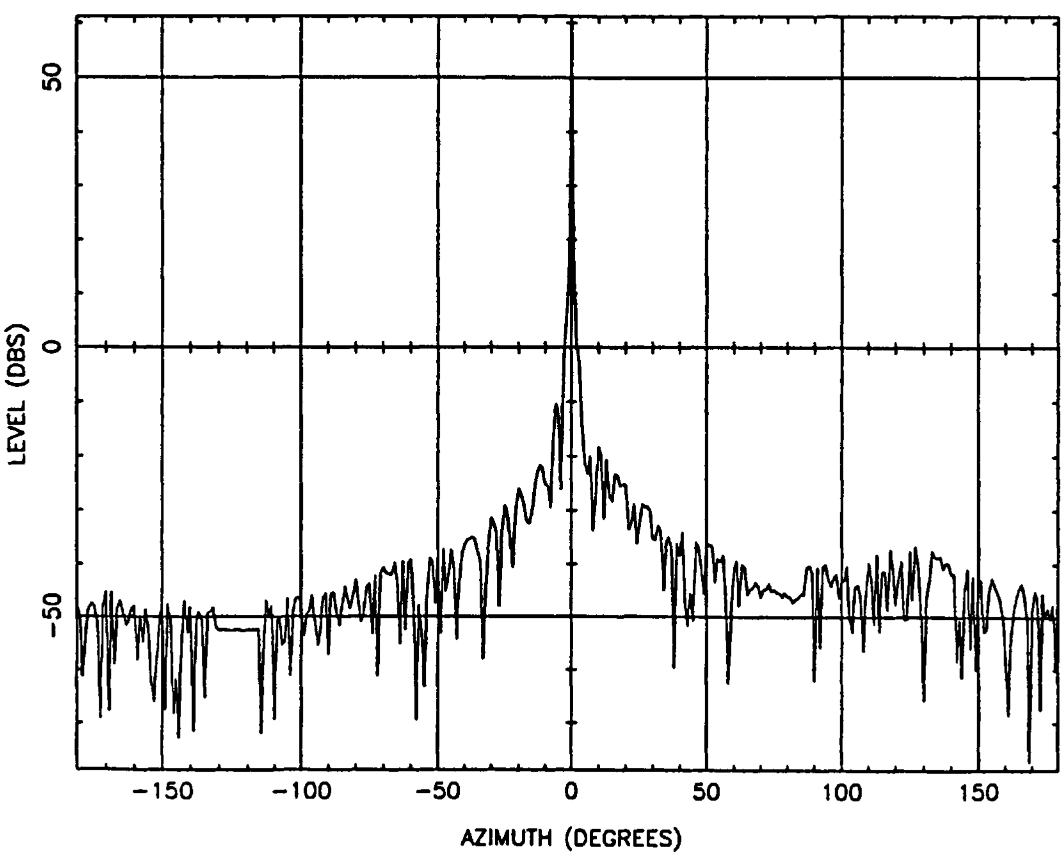

(d) 80° Plane

Fig. 5. Pattern of 90-meter asymmetric antenna at 1.4 GHz.

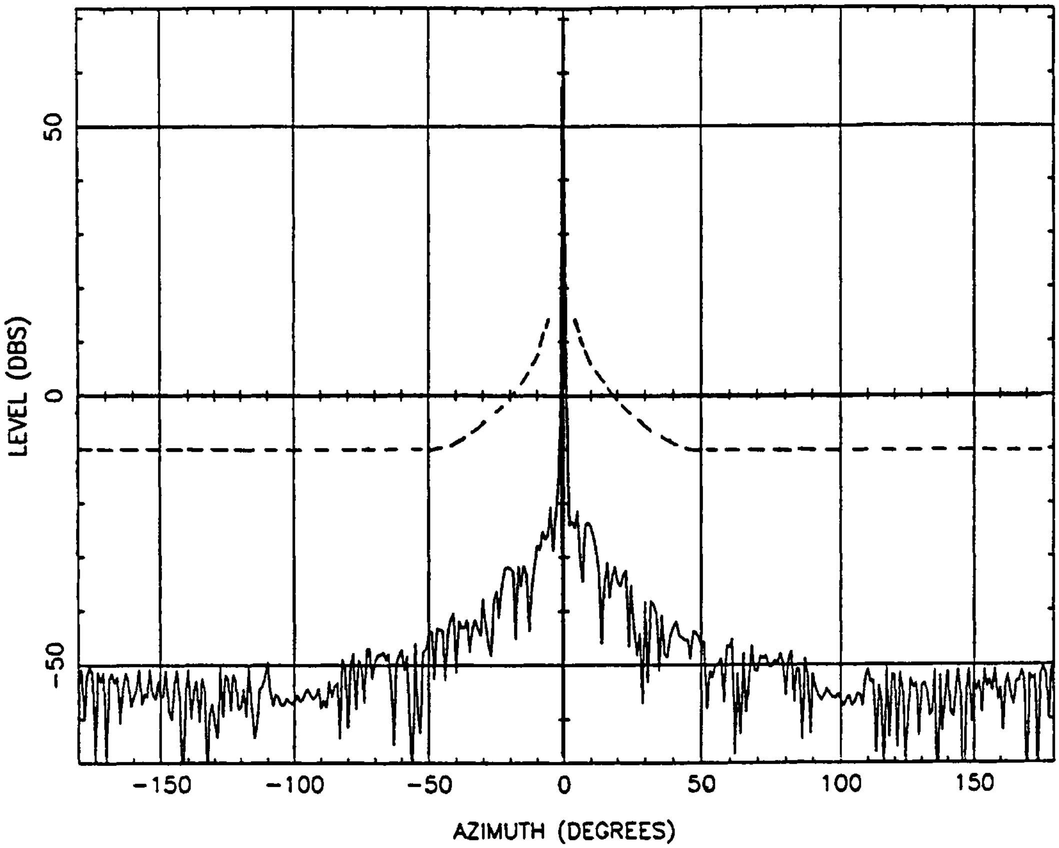

(a) Asymmetric (0°) Plane

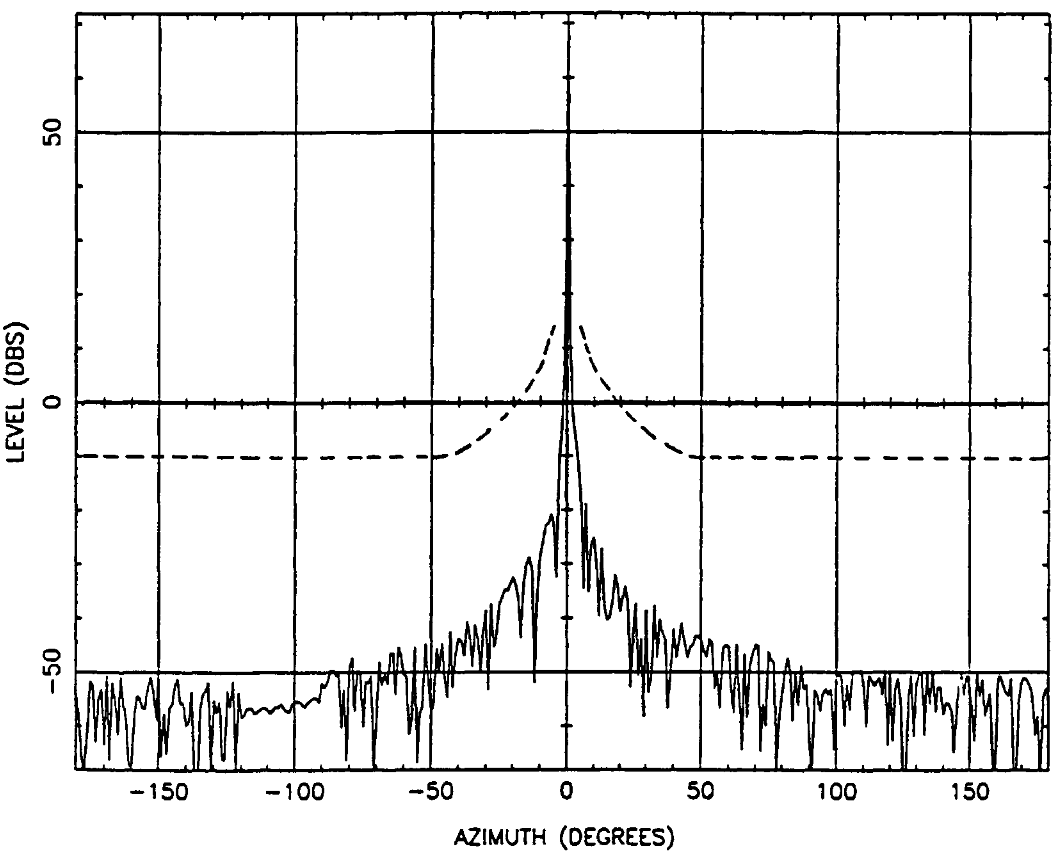

(b) 30° Plane

Fig. 6. Pattern of 90-meter asymmetric antenna at 4.8 GHz.

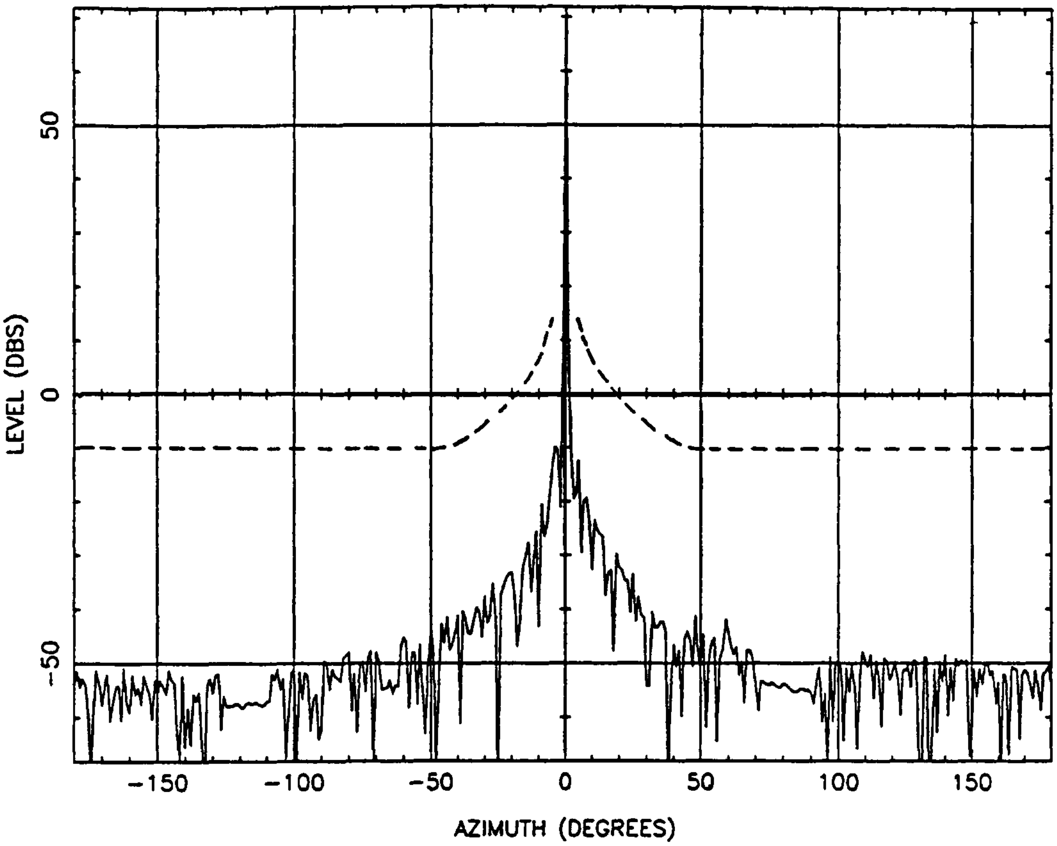

(c) 45° Plane

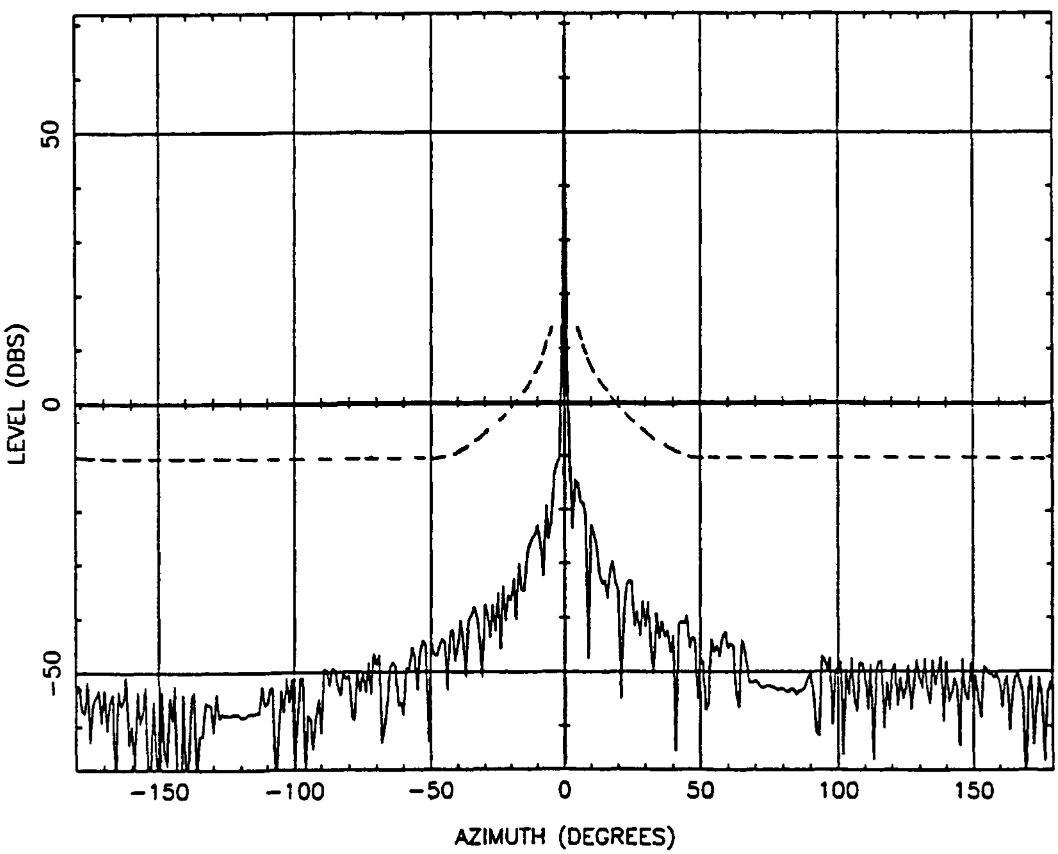

(d) 60° Plane

Fig. 6. Pattern of 90-meter asymmetric antenna at 4.8 GHz.